Research article

A pilot study comparing optical coherence tomography, radiography, clinical photography, and polarisation microscopy for studies of hypomineralisation disturbances in enamel

Josephine Solgaard Henriksen [a], Eva Lauridsen [b], Hans Gjørup [c], Hiba Al-Imam [d], Ted Lundgren [e], Nina Sabel [e], Agneta Robertson [e], Rubens Spin-Neto [f], Nuno Vibe Hermann [a,*]

[a] Pediatric Dentistry and Clinical Genetics, School of Dentistry, University of Copenhagen, Copenhagen, Denmark
[b] Resource Center for Rare Oral Diseases, Copenhagen University Hospital, Rigshospitalet, Copenhagen, Denmark
[c] Resource Center for Oral Health in Rare Diseases, Department of Maxillofacial Surgery, Aarhus University Hospital, Aarhus, Denmark
[d] Oral Rehabilitation and Dental Materials, School of Dentistry, University of Copenhagen, Copenhagen, Denmark
[e] Department of Pediatric Dentistry, Institute of Odontology, Sahlgrenska Academy, University of Gothenburg, Gothenburg, Sweden
[f] Department of Dentistry and Oral Health, Aarhus University, Aarhus, Denmark

ARTICLE INFO

ABSTRACT

Aim: To investigate the use of optical coherence tomography (OCT) as a tool to assess general and localised hypomineralisation defects in the enamel.

Design and Materials: Ten extracted permanent teeth (four teeth with localised hypomineralisation, four teeth with general hypomineralisation, and two healthy controls) were used in this study. In addition, four participants who underwent OCT served as living controls for the extracted teeth.

Methods: The OCT results were compared with clinical photographs, digital radiographs, and polarising microscopy images of tooth sections (considered the gold standard) to determine the method with the most accurate information regarding the extent of enamel disturbances: 1) visibility of enamel disturbance (visible yes/no); if yes, 2) extent of the disturbance in the enamel; and 3) determination of the plausible involvement of the underlying dentin.

Results: OCT was more accurate than digital radiography and visual assessment. OCT could provide information about the extent of localised hypomineralised disturbances in the enamel that was comparable to that with polarisation microscopy of the tooth sections.

Conclusion: Within the limitations of this pilot study, it can be concluded that OCT is suitable for investigating and evaluating localised hypomineralisation disturbances; however, it is less useful in cases with generalised hypomineralisation of the enamel. In addition, OCT complements radiographic examination of enamel; however, more studies are necessary to elucidate the full extent of the use of OCT in case of hypomineralisation.

---

1. Introduction

Hypomineralisation disturbances in the enamel have varying aetiologies, ranging from generalised disturbances of genetic origin to localised disturbances such as those caused by trauma or molar incisor hypomineralisation. A major clinical challenge in rehabilitating teeth with enamel defects (irrespective of their origin) is assessing the quality and depth of the involved tissue. Currently, the treatment choice is mainly based on visual assessment (inspection by the naked eye) and routine two-dimensional (2D) radiographs. However, these methods do not provide adequate information to clinicians regarding enamel quality and the extent of the defect. Thus, treatment is often based on an arbitrary estimation of enamel quality and extent of the hypomineralised area. This limitation may lead to diagnostic errors and treatment failure. New techniques that provide clinicians with this type of information are of interest and should be thoroughly evaluated.

Optical coherence tomography (OCT) is a non-invasive, non-radiation imaging technique based on differences in optical tissue properties and was first reported by Huang et al. [1]. OCT has revolutionised ophthalmology over the past 10 years and has been used to explore pathological changes in the retina [2,3]. OCT generates real-time 2D cross-sectional images with a high spatial resolution using near-infrared light waves. The technique is broadly considered analogous to ultrasound imaging; however, instead of sound waves, OCT uses light waves and is better suited for imaging near-surface structures, which makes it possible to capture structural details that are not possible with conventional radiography [4–7]. Depending on the structure being imaged, the effective imaging/penetration depth of OCT can reach up to 5 mm [8]. In 1998, the first *in vivo* images of dental hard and soft tissues were acquired using OCT [9]. Since then, this technique has undergone significant developments. OCT has shown excellent potential in research and clinical applications as it is considered a prospective diagnostic tool in dentistry to help dentists locate morphological changes in dental soft and hard tissues more accurately and rapidly [10].

Dental OCT has already proven useful in identifying cracks, microleakage around restorations, initial carious lesions, periodontal disease, and oral cancer [10–17]. Recently, hypomineralisation disturbances have been investigated in primary and permanent dentitions [5,10,11,13].

In this pilot study, we aimed to investigate the use of OCT as a clinical tool to assess hypomineralisation defects in the enamel. For this purpose, OCT images were compared with clinical photographs, radiographs, and polarising microscope images of tooth sections.

2. Material and methods

2.1. Materials

All teeth were collected in Denmark, and patient consent was obtained. The study followed the guidelines of the Declaration of Helsinki 1964 (https://www.wma.net/what-we-do/medical-ethics/declaration-of-helsinki/doh-jun1964/), and the material was anonymised and collected over several years. Thus, according to Danish ethical laws, approval from an ethical research committee was not required.

Ten extracted permanent teeth and four participants were included in this study. Four of the 10 teeth demonstrated hypomineralisation sequelae due to previous trauma in the primary dentition (TS), four were affected by amelogenesis imperfecta (AI), and two were considered healthy controls as assessed by clinical evaluation (Table 1).

The four included participants represented the three "conditions" demonstrated in the extracted teeth, namely TS (one participant), AI (two participants), and healthy control (one participant).

The participants were included to reveal plausible visible differences between OCT scans of extracted nonvital teeth and living vital teeth.

2.2. Methods

For each tooth, visual examination and scoring were performed in addition to OCT, clinical photography, digital radiography, and polarising microscopy of tooth sections. Finally, the different methods were compared to determine the method that provided the most accurate information regarding the quality and extent of the enamel defect. Polarising microscopy of tooth sections was considered the gold-standard method. Details about the methods and assessment procedures are described below, and an overview is provided in Table 2A–C.

Table 1
Distribution of the 10 teeth according to the clinical diagnosis. The mDDE codes are based on visual assessment.

Teeth (N = 10)	mDDE index code
Amelogenesis imperfecta = 4	6
- Hypomaturation: 2	
- Hypocalcification: 2	
Traumatized teeth = 4	0, 1, 4, 8, 9, B
Healthy control teeth = 2	0, 1, 4

mDDE, modified developmental defects of enamel.

During the evaluation, each surface was divided into smaller areas/parts/quadrants to ensure that the same area was evaluated using different imaging techniques. The lingual and facial surfaces were divided into nine equal-sized quadrants coded 1–9 (Table 2A). The evaluation was performed twice for each technique to estimate the method error.

2.2.1. Storage of teeth

All extracted teeth were stored in closed containers with formaldehyde (10% formaldehyde in phosphate-buffered saline [PBS]; pH 7.2). The teeth were embedded in acrylic blocks, replicating their position in the oral cavity, and the relevant surfaces (facial, mesial, lingual, and distal) were marked on the acrylic blocks. The formaldehyde in the containers was replaced with 0.9% sodium hypochlorite after the teeth were systematized and fixed into blocks of acrylic resin.

Immediately before testing, the teeth were removed from their container and dried.

2.2.2. Clinical images

All images were taken on the same day using a Canon EOS camera equipped with a ring light flash (Canon Ringblitz MR-14 EX®), and all teeth were placed against the same blue background during exposure. The focus operation was set to manual focus (MF). The distance between the object and the camera was approximately 25–30 cm. All artificial lights in the room were switched off. The teeth were placed in red wax and all surfaces were photographed (occlusal, facial/buccal, distal, lingual/palatal, and mesial). The modified developmental defect of enamel (DDE) index was used to categorise the enamel lesions [18].

2.2.3. Visual clinical assessment

Visual clinical assessment was performed by an experienced observer using the modified DDE (mDDE) index. The defects were categorised into demarcated opacities (code 1–2), diffuse opacities (code 3–6), hypoplasia (code 7–9), and combinations (codes A) [18, 19].

2.2.4. Digital radiographs

A rectangular X-ray tube was placed approximately 5 cm away from the target object. Exposure setting for the teeth: BW child: 70 kV, 8 mA, P.125 s. Two radiographic images were obtained for each tooth (facial and approximal) such that the entire tooth was visible on the image.

2.2.5. OCT

A swept-source OCT device (IVS-300®, Santec Corporation, Aichi, Japan) with a coherence length >150 nm was used. The scanner was equipped with a laser (wavelength: 1310 ± 30 nm) with an axial resolution ≤ 12 µm and a lateral resolution of 22 µm. The working distance between the object and the probe was ≤ 10 mm [10–12].

2.3. Procedure during scanning

The handheld OCT probe was mounted onto a movable arm and placed in a specific fixed position (the angulation was fixed during scanning) to maintain reproducibility and image stability. The teeth (fixed in acrylic blocks) were then transferred from the storage medium, and the excess liquid was removed before they were placed in a self-made holder. The distance between the tooth and OCT probe was as small as possible and not >1 cm. All scans were performed from the right to left side. The scan started from the first visible portion of the tooth surface until the surface was no longer visible. Cross-sectional images, called B-scans, were obtained at a distance of 2 mm between each frame. The number of B-scans for each surface depended on the width of the tooth surface. Each tooth was scanned twice, a few days apart, to exclude the influence of the scanning procedure on the results. The occlusal surfaces were not scanned due to their complex morphology. Because the entire tooth surface is not visible on B-scans, they reflect only a selected area of the surface. Clinically visible hypomineralised areas determine the reference point of the scan. The B-scans were processed using ImageJ software (ImageJ, version 1.50a; Wayne Rasband, NIH, USA).

2.4. OCT evaluation

All visible enamel disturbances on the B-scans were noted (the location and its boundaries [diffuse or well-defined]). The extent (width and depth) of well-defined enamel disturbances were noted as either involving: 1) only the enamel, 2) from the enamel surface to the dentino-enamel junction (DEJ), or 3) from the enamel surface into the dentin layer.

As mentioned above, OCT can help visualise the differences in tissue optical properties based on the effects of optical absorption

Table 2A
The codes for each area of the facial and lingual surfaces.

Mesial	Incisal/Occlusal			Distal
	1	2	3	
	4	5	6	
	7	8	9	
	Cervical			

Table 2B
Overview of assessment procedures [10–12,19,21,21].

Overview and details of assessment procedures				
Visual assessment (The modified developmental defects of enamel (mDDE) index -Defects were categorised as: a) demarcated opacities (code 1–2), b) diffuse opacities (code 3–6), c) hypoplasia (code 7–9), and d) combinations (code A-D).	Clinical images (Figs. 1A–4A) (Canon EOS camera equipped with a ring light flash (Canon Ringblitz MR-14 EX®)) -The teeth were placed in red wax and all surfaces were photographed (occlusal, facial/ buccal, distal, lingual/palatal, and mesial surfaces). -The focus operation was set to manual focus. -The distance between the object and the camera was 25 cm. -All artificial lights in the room were turned off. -Same blue background during exposure.	Digital radiographs (Figs. 1B–4B)	OCT scanning (Figs. 1C–4C) (IVS-300®, Santec Corporation, Aichi, Japan) -Scanner: A swept-source OCT device -Coherence length of >150 nm -The scanner was equipped with a laser (wavelength: 1310 ± 30 nm) with an axial resolution of ≤ 12 μm and a lateral resolution of 22 μm. -Working distance between the object and probe was ≤ 10 mm. See Table 2C for details in OCT-scanning procedure of extracted and living in situ teeth.	**Polarising microscopy** (Olympus BX50 polarising light microscope (Olympus, Tokyo, Japan)) *-Prior to polarisation microscopy, the undecalcified teeth were*: a) Rinsed in 70% ethanol b) Mounted for cutting orientation, and re-embedded in EpoFix (Struers, Denmark). *-After polymerisation, the teeth were:* a) Longitudinally ground cut with a low-speed diamond saw (Leica, Wetzlar, Germany) into 130-μm thick sections. b) Glued to objective glasses using Technovit (Kulzer, Germany). c) Air-dried d) Examined at 20× magnification using a λ-filter. D) Photographed and analyzed using the Leica Application Suite (Leica Microsystems AG, Heerbrugg, Switzerland). *-Histological sections of the teeth (* Figs. 1f–4f): a) Images were analyzed using NIS-Elements D image analysis software, version 5.01. b) Enamel morphology, translucency, and birefringence were assessed using a standard protocol.

and scattering [11]. The resulting images, called B-scans, represent 2D data shown in a cross-sectional plane through the tissue shown as a grayscale image, where each pixel indicates either high reflectivity (white) or low reflectivity (black) [8,11].

Enamel and dentin have different optical properties due to their different structural compositions, which makes it possible to differentiate between the two hard tissues on the scan. Sound dentin and enamel appear homogeneously greyish. Because the OCT scanner has a penetration depth of only a few millimetres, deeper structures appear black. The DEJ appears as a dark border between the enamel and dentin layer [10,11].

Hypomineralised enamel is characterised by a deficiency of minerals, which results in increased enamel porosity. The mineral content (or mineral loss) of the hypomineralised enamel affects how the hypomineralised area appears on the B-scan/OCT scan. Mineral changes in the enamel change light propagation through the teeth, which means that optical absorption and scattering in this specific area is altered, resulting in a visible change in the enamel on the B-scan [7,11,14,17,20].

2.5. Control participants

All four healthy control participants were treated according to the 1964 Helsinki Declaration, and all agreed to be included in this study and to the publication of the collected data (https://www.wma.net/what-we-do/medical-ethics/declaration-of-helsinki/doh-jun1964/).

All participants were seated in a chair during the scanning. Owing to the probe size of the OCT scanner, it was only possible to scan from the left to the right premolars (in both the maxilla and mandible). Two B-scans were obtained per tooth (facial side): one incisal and one gingival. OCT scanning was performed by two trained investigators.

2.5.1. Polarising microscopy
Prior to polarising microscopy, the undecalcified teeth were rinsed in 70% ethanol, mounted for cutting orientation, and re-embedded in EpoFix (Struers, Denmark). After polymerisation, the teeth were sectioned longitudinally using a low-speed diamond bur (Leica, Wetzlar, Germany) into 130-μm-thick sections [21]. The sections were glued to objective glasses using Technovit (Kulzer, Germany). All sections of teeth were examined dry in air and after water imbibition in a Olympus BX50 polarising light microscope (Olympus, Tokyo, Japan) at ×20 magnification using a λ-filter (a modum [22]). The sections were then photographed and analyzed using the Leica Application Suite (Leica Microsystems AG, Heerbrugg, Switzerland) [23].

Table 2C

Overview of steps in OCT-scanning procedure in extracted versus in situ living teeth [7,8,10,11,12,14,17,20,27].

Overview of steps in OCT-scanning procedure in extracted versus *in situ* living teeth			
Procedure for OCT of extracted teeth	Procedure for OCT in the mouth	OCT registration	Explanation of the OCT B-scans (Figs. 1C–4C)
a) The handheld OCT-probe was mounted onto a movable arm and placed in a specific fixed position (the angulation was fixed during the scanning) to maintain reproducibility and image stability. b) The teeth (fixed in acrylic blocks) were then transferred from the storage medium and placed in a self-made holder. c) The distance between the OCT probe and tooth was ≤1 cm. All scans were performed from right to left. d) Cross-sectional images, called B-scans, were taken with each frame 2 mm apart across the surface. The occlusal surfaces were not scanned owing to their complex morphology. Since the entire tooth surface was not visible on the B-scans, the B-scans reflected a selected area of the surface. Clinically visible hypomineralised areas determined the reference point of the scan. e) The B-scans were post-processed using ImageJ software (ImageJ, version 1.50a; Wayne Rasband, NIH, USA).	a) The participants were seated in a chair during the scanning. b) It was only possible to scan from the left to the right premolars (both the maxilla and mandible) owing to the probe size of the OCT scanner. c) Two B-scans were obtained per tooth (facial aspect), one incisally and one gingivally. d) OCT scanning was performed by two trained clinicians from the project group.	-*Healthy enamel:* a) The thickness of the healthy/normal enamel was measured from the enamel surface to the dentino-enamel junction (DEJ). b) The measurement was performed on the B-scan of a given surface. If the DEJ was not visible, the measurement was not performed. -*Enamel disturbances:* a) All visible enamel disturbances on the B-scans were noted (the location and its boundaries [diffuse or well-defined]). b) The extent (width and depth) of well-defined enamel disturbances were measured using dedicated software (ImageJ, NIH, USA), whereas diffuse enamel disturbances were noted as present or absent. c) The measurements in pixels were converted into micrometres by multiplying the number of pixels with the corresponding pixel size (16.84 µm/pixel on the z-axis or 6,72 µm/pixel on the y-axis) and dividing it with the refractive index (n) of enamel (n = 1.631), and the refractive index of hypomineralised enamel in water was set to (n = 1,33).	a) B-scans represent 2D data in a cross-sectional plane through the tissue shown as a grayscale image b) Each pixel indicates either high reflectivity (white) or low reflectivity (black). c) Enamel and dentin have different optical properties owing to their different structural compositions. d) Normal enamel and dentin appear homogeneously greyish. e) Penetration depth is only a few millimetres; thus deeper structures appear black. f) The DEJ appears as a dark borderline between the enamel and dentin. g) Hypomineralised enamel is characterised by a deficiency of minerals, which results in increased porosity of the enamel. Mineral changes in the enamel change the light propagation through the teeth, which means that the optical absorption and scattering will be altered in this specific area and change the appearance of the enamel in the B-scan.

2.6. Histological sections of the teeth

The images were analyzed using the NIS-Elements D image analysis software, version 5.01. Dental enamel morphology, translucency, and birefringence were assessed using standard protocols.

3. Results

Fig. 1 (A-D) depicts the normal control tooth, Fig. 2 (A-D) depicts the teeth affected by AI, and Fig. 3 (A-D) and 4 (A-D) depict permanent teeth with hypomineralisation sequelae after trauma to the primary dentition.

3.1. Visual examination

Clinical visual variations in enamel hypomineralisation due to previous trauma in the primary dentition were observed. The extent of hypomineralisation in the underlying dentin could not be determined by visual inspection.

All teeth with AI demonstrated discoloured yellow-brown enamel. Teeth with hypomaturation AI were characterised by normal enamel thickness and a smooth surface.

Teeth with hypocalcification AI had hypomineralised and hypoplastic enamel; the enamel surface appeared rough and pitted with ridges, and the enamel was thin and irregular.

Therefore, it was not possible to determine whether the underlying dentin was affected. All teeth with AI were assigned an mDDE code of 6 (Table 1).

3.2. Radiographic examination

In most teeth affected by trauma, it is challenging to identify and diagnose clinically observed hypomineralised areas in the enamel on radiographic images.

Teeth with hypomineralised AI (hypomaturation type) showed a normal radiographic contrast between the enamel and dentin. In contrast, teeth with a combination of hypomineralised and hypoplastic AI (hypocalcification type) showed almost equal radiopacity of both the enamel and dentin, and the thickness of the enamel was markedly reduced.
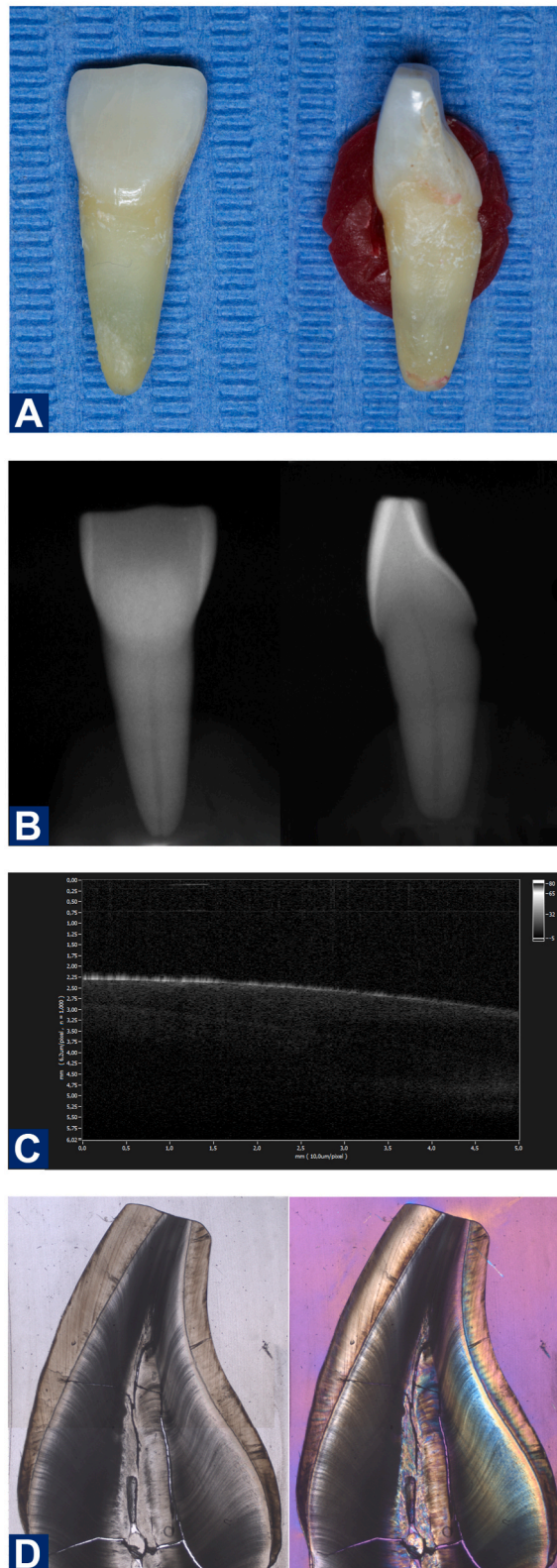
Fig. 1. Example showing a control tooth (incisor): A) Clinical photo. B) Radiograph. C) B-scan of quadrant 5 on the facial side. D) Polarising microscopy image of tooth. Left: white light. Right: polarized light.
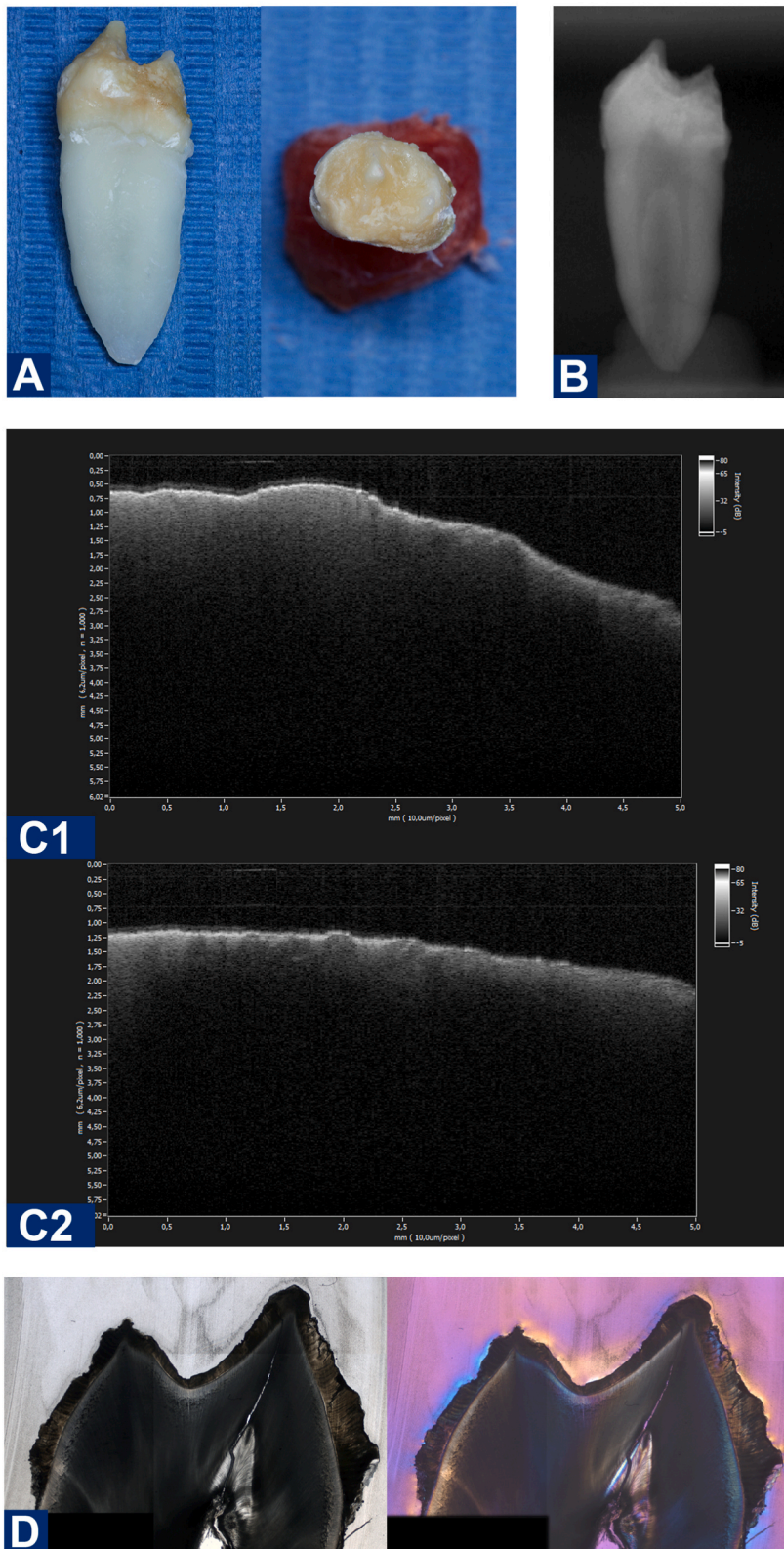
Fig. 2. Example showing a tooth with AI (hypocalcification subtype): A) Clinical photo of the mesial surface. B) Radiograph. C) c1: B-scan of the facial surface c2: B-scan of the lingual surface. D) Polarising microscopy image of the tooth. Left: white light. Right: polarized light.
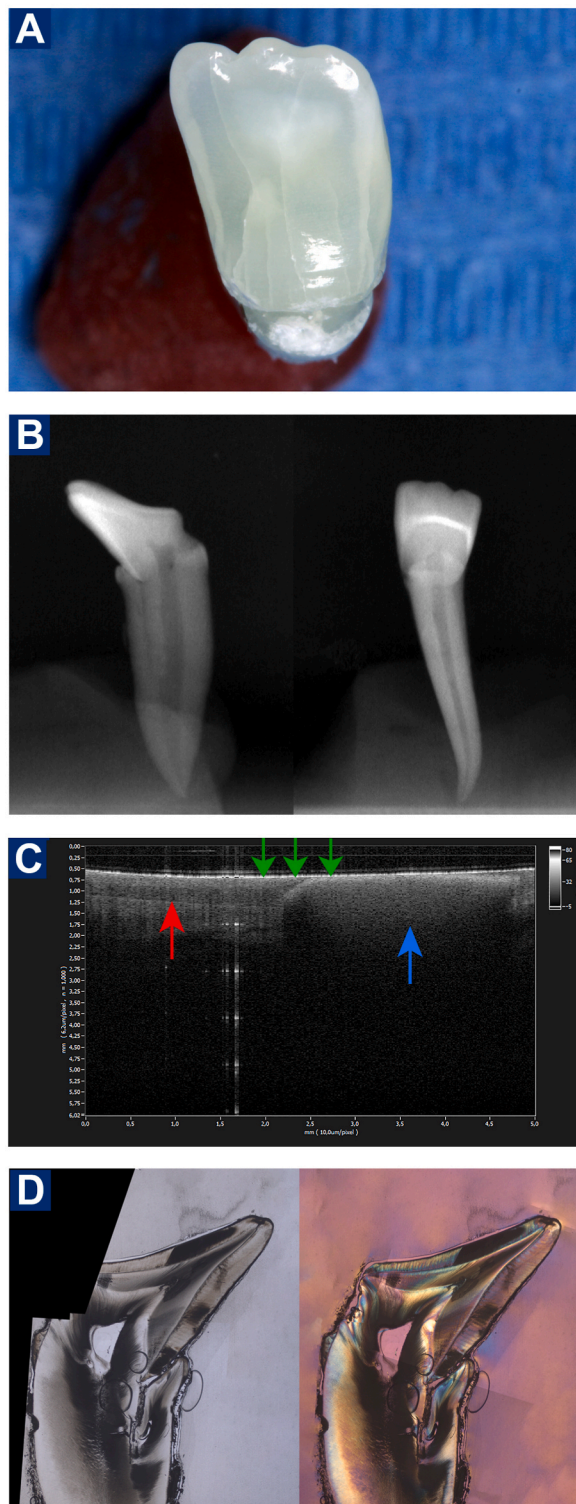
Fig. 3. Example showing a permanent tooth with a developmental disturbance in the enamel (white opacity) and tooth shape caused by trauma to the tooth bud during development (trauma to the primary tooth): A) Clinical photos. B) Radiograph. C) B-scans of the facial surface. In the B-scan, the incisal edge of the tooth is visible, and the scans are obtained from the mesial [1] to distal [4] aspect. The blue arrow points to the hypo-mineralised area in the enamel, the red arrow points to the dentino-enamel junction (DEJ), and the green arrow points to the enamel surface. D) Polarising microscopy image of the tooth. Left: white light. Right: polarized light. (For interpretation of the references to colour in this figure legend, the reader is referred to the Web version of this article.)
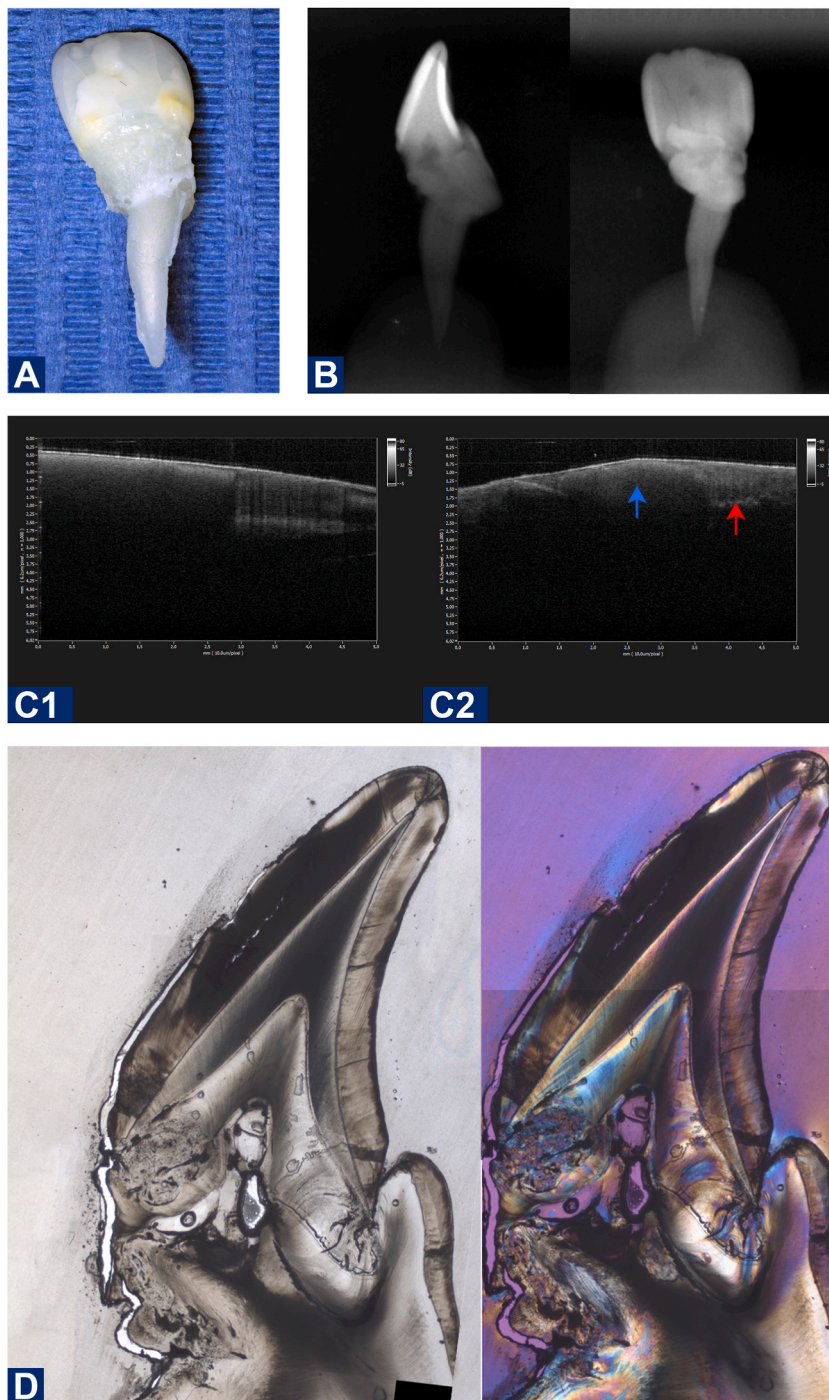
Fig. 4. The figure shows a tooth that has been exposed to trauma during development (trauma to the primary tooth), which has led to a developmental disturbance in the enamel of the permanent successor (crown dilaceration). A) Clinical photos. Several white and yellow well-defined opacities are seen on the facial surface. B) Radiograph. C) B-scans of the facial surface C1) a B-scan of the incisal part of the tooth; a well-defined bright area in the enamel is observed; C2) a B-scan of the cervical part of the tooth; a well-defined area in the enamel is visible near the cementoenamel junction (CEJ). On the B-scan (C2), the blue arrow points at the hypomineralised area in the enamel and the red arrow points at the dentino-enamel junction (DEJ). D) The histological section on the left side is seen in white light, and in polarized light on the right side. (For interpretation of the references to colour in this figure legend, the reader is referred to the Web version of this article.)

3.3. OCT examination

All healthy control teeth showed distinct boundaries between the hard tissues. Fig. 1C depicts the B-scan of a healthy tooth.

The hypomineralised areas in all teeth with hypomineralisation varied in appearance on the OCT image and ranged from diffuse dark areas to well-defined, bright areas in the enamel. Accordingly, in three out of four teeth with sequelae after trauma, the OCT image showed a well-defined, bright area in the dental enamel located at the same site as the clinically observed opacity. However, in the fourth tooth, the opacity was shown as diffuse dark areas on the OCT image. We found that the defects affected the entire enamel layer. Whether the hypomineralised area extended into the dentin layer could not be determined from the OCT scans.

Fig. 4 (A-D) shows a tooth exposed to trauma during development. The opacities are easily observed clinically, where several well-defined white and yellow opacities are seen on the facial surface. The two B-scans show the incisal part (4-C1) and cervical part (4-C2) of the tooth. In both B-scans, a well-defined area in the enamel was visible and differed from the surrounding healthy enamel.

In cases with generalised hypomineralisation disturbances (AI), OCT cannot detect the borders of hypomineralisation. It was challenging to visualise a distinction between different hard tissues using OCT in the patients with AI regardless of the sub-diagnosis, as the DEJ was not visible or only visible in some areas, making it challenging to determine the transition between the enamel and dentin. Other than that, it was evident that the enamel layer was uneven.

Fig. 2(C1 and C2) shows the randomly selected B-scans (lingual and facial surfaces) of a tooth affected by AI. It was difficult to visualise a distinction between the different hard tissues on the B-scans. Compared to a healthy control tooth (Fig. 1C), the DEJ was not visible or only visible in some areas, making it difficult to determine the transition between enamel and dentin.

3.4. Polarisation microscopy

In the teeth affected by trauma, clinically visible opacities within the enamel appeared as non-translucent areas. In most cases, the non-translucent areas appeared to extend almost throughout the entire enamel thickness. The birefringence colour of enamel opacities did not seem to correlate with the depth of the hypomineralised area, often extending through the entire thickness of the enamel regardless of the location of the opacity (Figs. 3D and 4D).

In conjunction with dilacerations, invaginations were observed on the lingual aspect, extending into the dentin. In general, the enamel thickness was normal, with local non-translucencies in the dilacerated areas.

In the teeth affected by AI, the thickness of the enamel varied, with varying degrees of absence of substance. The enamel was mostly non-translucent with nondispersive birefringence. The enamel was also mostly thin, irregular, and rough, with some locations showing a normal thickness and appearance. Differentiating enamel prisms was challenging, and incremental lines could not be observed. Only one of the four teeth with AI is shown (Fig. 2(c1 and C2)) as all B-scans of the teeth with AI appeared alike.

4. Discussion

The advantages and disadvantages of the methods (visual examination, radiography, polarisation microscopy, and OCT) are listed in Table 3 [10].

4.1. Visual examination

Visual clinical assessment is undoubtedly an essential part of the dentist's overall assessment of a patient's teeth. The examination is performed by the naked eye and is based on the dentist's professional knowledge and experience; it only requires a few instruments, is non-radiative, and bears low cost. However, one must assume that variations exist in what one visualizes clinically depending on who is examining the patient.

Dabiri et al. [19] examined dentists' ability to correctly identify and classify different types of DDE. The respondents had to score 36 images using the mDDE index, based on a short training table with images. The results of the survey (348 in total) showed pronounced

Table 3
Schematic overview of the advantages and disadvantages of the different methods.

Method	Advantages	Disadvantages
Visual inspection	No cost	Only surface information
	Non-ionising	
	Easy and fast method	
Radiography	Low cost	Tooth structure may be superimposed
	Broad measurement range	Ionising radiation
	The equipment is already available at most dental clinics	Two-dimensional images
Optical coherence tomography	High spatial resolution	Limited penetration depth and scanning range
	Non-invasive, real-time images	The device is expensive
	Three-dimensional image reconstruction is available	
	Non-ionising	
Microscopy of histological sections	Gold standard method, high spatial resolution of tissues	Only possible on extracted teeth
	Differentiates mineralisation aberrations	Expensive
		Time consuming

variation in correct responses for each image, ranging from 41% to 97%, for each category of the mDDE index. The study concluded that dental providers need enhanced training and calibration to identify different types of DDE.

The teeth in our study, which had been exposed to trauma, varied more in their clinical appearance; therefore, a greater range of mDDE codes was expected as it is well known that the type of trauma (impact and direction of the force), the patient's age, and the developmental stage of permanent tooth germ at the time of trauma has an impact on the severity of the subsequently observed sequelae in the permanent tooth [24].

4.2. Radiographic examination

Conventional 2D radiographic examination has limitations due to the ionising radiation exposure of the patient and 2D summation imaging of a three-dimensional object (the tooth). This makes it difficult to localise specific structural features, such as minor local changes in mineralisation in the enamel; this, can thus, lead to diagnostic errors. From a diagnostic perspective, X-ray imaging is, therefore, not an ideal method for evaluating localised disturbances [25].

In the cases from our study where a general hypomineralisation disturbance was found, it seemed that the radiographic images could only demonstrate whether the dental enamel was affected and whether the whole enamel layer was involved. In this sense, a radiograph confirms what one sees clinically and may be helpful in differentiating between subtypes of AI.

Studies have reported that in bitewing images, the mineral loss due to demineralisation caused by a carious lesion must be approximately 35% on the proximal surface of the tooth before it can be observed radiologically, and the relationship between mineral loss and radiological visibility depends on the overall thickness of the enamel in the studied area [26]. Although this has not been confirmed in any studies, there is no reason to believe that the level of mineral loss before detection on X-rays should be different in the case of hypomineralisation compared to that in cases of demineralisation caused by caries. This may explain why some of the teeth in our sample did not show any radiological signs of hypomineralisation, despite hypomineralisation being observed clinically.

4.3. Polarising microscopy

Polarising microscopy is a suitable method to analyse mineralisation disturbances in dental hard tissues as even minor variations and differences in crystal directions can give rise to visible colour variations in images. Thus, it serves as the gold standard in validation studies. However, a major drawback of this method is that it can only be used in cases of extracted teeth.

4.4. OCT

One of the four teeth with sequelae after trauma showed a diffuse dark area in the dental enamel on the B-scans, whereas the other three showed well-defined areas in the enamel. Further studies are needed to determine the reason behind this.

Several studies have reported a distinction between sound and demineralised enamel [11,12,20]. Demineralised enamel appears brighter on grayscale OCT imaging, which is caused by two main principles: increased light scattering in porous demineralised tissue and depolarisation of incident light by demineralised tissue [11,12]. There are many similarities between demineralised and hypomineralised enamel, such as the loss of minerals and a more porous enamel structure, which is why these two principles probably also explain why hypomineralised enamel in some cases appears brighter/lighter than sound enamel.

A limitation of the OCT technique is that only materials that transmit/backscatter light may be assessed. Teeth with metal-based restorations or other materials with high refractive indices are not suitable for OCT scanning. Furthermore, distortion on B-scans may occur occasionally owing to the prominence/curvature of the teeth [12].

Future studies may choose to obtain more OCT B-scans of each surface and reduce the distance between the B-scans to <2 mm. By obtaining more scans per surface, one should expect to obtain more detailed insights into the enamel structure. Notably, the quality and structure of enamel can vary from person to person; however, these minor variations are not expected to significantly affect the appearance of the B-scan image.

In addition, measurements of the extent of the hypomineralised area can be performed in future studies, by comparing these measurements with their respective clinical extent. This could provide clinicians with knowledge that cannot be obtained from clinical observations, and which is considered very difficult to determine from radiographs.

When using an OCT scanner in the clinic, it is crucial to use a modified clinical version of the apparatus. The probe design of our OCT scanner was mainly for laboratory purposes, which made scanning directly in the oral cavity very challenging, especially when scanning the molars.

5. Conclusion

OCT enables real-time imaging in a non-contact and non-invasive manner to a depth of up to 2−3 mm in the enamel and can identify structural details as small as ≤12 μm in the tooth. These properties make OCT a suitable tool for detecting subsurface changes and a plausible and useful method in modern dental diagnostics.

The present pilot study shows that OCT may be particularly interesting for investigating and evaluating localised hypomineralisation disturbances, whereas it is probably less useful in cases of generalised enamel hypomineralisation. In localised hypomineralisation disturbances, OCT may provide information about the quality of the dental enamel and the extent of the depth of the hypomineralised area, which is in contrast to information from radiographs that only provides summation images of the condition.

Knowledge about the depth of hypomineralisation is important during treatment for planning the best treatment strategy and, in the end, providing the best prognosis for the patient.

The limitations of this study include the small sample size and the qualitative nature of the study. Future studies investigating all aspects of the usefulness of OCT in hypomineralised teeth should include larger sample sizes to verify and quantify all the details.

Author contribution statement

Josephine Solgaard: Conceived and designed the experiments; Performed the experiments; Analyzed and interpreted the data; Contributed reagents, materials, analysis tools or data; Wrote the paper.

Eva Lauridsen: Conceived and designed the experiments; Analyzed and interpreted the data; Wrote the paper.

Hans Gjørup: Contributed reagents, materials, analysis tools or data; Wrote the paper.

Hiba Al-Imam: Contributed reagents, materials, analysis tools or data.

Ted Lundgren; Nina Sabel; Agneta Robertson; Rubens Spin-Neto: Performed the experiments; Analyzed and interpreted the data; Wrote the paper.

Nuno Vibe Hermann: Conceived and designed the experiments; Analyzed and interpreted the data; Contributed reagents, materials, analysis tools or data; Wrote the paper.

Funding statement

Data availability statement

Data will be made available on request.

Declaration of interest's statement

The authors declare no competing interests.

References

[1] D. Huang, E.A. Swanson, C.P. Lin, J.S. Schuman, W.G. Stinson, W. Chang, M.R. Hee, T. Flotte, K. Gregory, C.A. Puliafito, Optical coherence tomography, Science (New York, N.Y.) 254 (5035) (1991) 1178–1181, https://doi.org/10.1126/science.1957169.

[2] A.H. Kashani, C.L. Chen, J.K. Gahm, F. Zheng, G.M. Richter, P.J. Rosenfeld, Y. Shi, R.K. Wang, Optical coherence tomography angiography: a comprehensive review of current methods and clinical applications, Prog. Retin. Eye Res. 60 (2017) 66–100, https://doi.org/10.1016/j.preteyeres.2017.07.002.

[3] R.F. Spaide, J.G. Fujimoto, N.K. Waheed, S.R. Sadda, G. Staurenghi, Optical coherence tomography angiography, Prog. Retin. Eye Res. 64 (2018) 1–55, https://doi.org/10.1016/j.preteyeres.2017.11.003.

[4] L.P. Choo-Smith, C.C. Dong, B. Cleghorn, M. Hewko, Shedding new light on early caries detection, Tex. Dent. J. 126 (2) (2009) 152–159.

[5] M. Machoy, J. Seeliger, L. Szyszka-Sommerfeld, R. Koprowski, T. Gedrange, K. Woźniak, The use of optical coherence tomography in dental diagnostics: a atate-of-the-art review, J. Health. Eng. (2017), 7560645, https://doi.org/10.1155/2017/7560645, 2017.

[6] R.A. Erdelyi, V.F. Duma, C. Sinescu, G.M. Dobre, A. Bradu, A. Podoleanu, Optimization of X-ray investigations in dentistry using optical coherence tomography, Sensors 21 (13) (2021) 4554, https://doi.org/10.3390/s21134554.

[7] J. Fujimoto, E. Swanson, The development, commercialization, and impact of optical coherence tomography, Investig. Ophthalmol. Vis. Sci. 57 (9) (2016), https://doi.org/10.1167/iovs.16-19963. OCT1–OCT13.

[8] R.A. Katkar, S.A. Tadinada, B.T. Amaechi, D. Fried, Optical coherence tomography, Dent. Clin. 62 (3) (2018) 421–434, https://doi.org/10.1016/j.cden.2018.03.004.

[9] B. Colston, U. Sathyam, L. Dasilva, M. Everett, P. Stroeve, L. Otis, Dental OCT, Opt. Exp. 3 (6) (1998) 230–238, https://doi.org/10.1364/oe.3.000230.

[10] Y.S. Hsieh, Y.C. Ho, S.Y. Lee, C.C. Chuang, J.C. Tsai, K.F. Lin, C.W. Sun, Dental optical coherence tomography, Sensors 13 (7) (2013) 8928–8949, https://doi.org/10.3390/s130708928.

[11] Y. Shimada, A. Sadr, Y. Sumi, J. Tagami, Application of optical coherence tomography (OCT) for diagnosis of caries, cracks, and defects of restorations, Curr. Oral Heal. Rep. 2 (2) (2015) 73–80, https://doi.org/10.1007/s40496-015-0045-z.

[12] H. Al-Imam, S. Michou, A.R. Benetti, K. Gotfredsen, Evaluation of marginal and internal fit of acrylic bridges using optical coherence tomography, J. Oral Rehabil. 46 (3) (2019) 274–281, https://doi.org/10.1111/joor.12746.

[13] M.T. Tsai, Y.L. Wang, T.W. Yeh, H.C. Lee, W.J. Chen, J.L. Ke, Y.J. Lee, Early detection of enamel demineralization by optical coherence tomography, Sci. Rep. 9 (1) (2019), 17154, https://doi.org/10.1038/s41598-019-53567-7.

[14] D.P. Popescu, M.G. Sowa, M.D. Hewko, L.P. Choo-Smith, Assessment of early demineralization in teeth using the signal attenuation in optical coherence tomography images, J. Biomed. Opt. 13 (5) (2008), 054053, https://doi.org/10.1117/1.2992129.

[15] Y. Zhou, Y. Shimada, K. Matin, A. Sadr, Y. Sumi, J. Tagami, Assessment of bacterial demineralization around composite restorations using swept-source optical coherence tomography (SS-OCT), Dent. Mater. : Off. Pub. Acad. Dent. Mater. 32 (9) (2016) 1177–1188, https://doi.org/10.1016/j.dental.2016.06.022.

[16] F. Kashirtsev, J. Tressel, J.C. Simon, D. Fried, High contrast imaging of dental fluorosis in the short wavelength infrared, J. Biophot. 14 (10) (2021), e202100145, https://doi.org/10.1002/jbio.202100145.

[17] Y. Shimada, M. Yoshiyama, J. Tagami, Y. Sumi, Evaluation of dental caries, tooth crack, and age-related changes in tooth structure using optical coherence tomography, Jap. Dent. Sci. Rev. 56 (1) (2020) 109–118, https://doi.org/10.1016/j.jdsr.2020.08.001.

[18] Commission On Oral Health, Research & epidemiology. Report Of An FDI Working group, A review of the developmental defects of enamel index (DDE Index), Int. Dent. J. 42 (6) (1992) 411–426.

[19] D. Dabiri, G.J. Eckert, Y. Li, K. Seow, R.J. Schroth, J. Warren, J.T. Wright, S. Zhao, M. Fontana, Diagnosing developmental defects of enamel: pilot study of online training and accuracy, Pediatr. Dent. 40 (2) (2018) 105–109.

[20] K. Al-Azri, L.N. Melita, A.P. Strange, F. Festy, M. Al-Jawad, R. Cook, S. Parekh, L. Bozec, Optical coherence tomography use in the diagnosis of enamel defects, J. Biomed. Opt. 21 (3) (2016), 36004, https://doi.org/10.1117/1.JBO.21.3.036004.

[21] J.G. Noren, Cutting mineralized hard tissues with the Leitz low-speed saw microtome, Leitz Mitt Tech 9 (1987) 49–52.

[22] N. Sabel, G. Klingberg, W. Dietz, S. Nietzsche, J.G. Norén, Polarized light and scanning electron microscopic investigation of enamel hypoplasia in primary teeth, Int. J. Paediatr. Dent. 20 (2010) 31–36, https://doi.org/10.1111/j.1365-263X.2009.01006 (x)).

[23] N. Sabel, A. Robertson, S. Nietzsche, J.G. Norén, Demineralization of enamel in primary second molars related to properties of the enamel, Sci. World J. (2012), 587254, https://doi.org/10.1100/2012/587254, 2012.

[24] J.O. Andreasen, F.M. Andreasen, L. Andersson, Textbook and Color Atlas of Traumatic Injuries to the Teeth, Wiley-Blackwell, Oxford, UK, 2018.

[25] A. Wenzel, M. Wiese, I. Sewerin, *Stråledoser. stråleskader, strålebeskyttelse - en orientering for tandlægestuderende og personale i tandlægepraksis (book)*, Munksgaard, Danmark, 2011.

[26] S. Mallya, L. Ernest, White and Pharoah's Oral Radiology, Elsevier, Amsterdam, Netherlands, 2018.

[27] Z. Meng, X.S. Yao, H. Yao, Y. Liang, T. Liu, Y. Li, G. Wang, S. Lan, Measurement of the refractive index of human teeth by optical coherence tomography, J. Biomed. Opt. 14 (3) (2009), 034010, https://doi.org/10.1117/1.3130322.